Aggregation Properties of Amphiphilic Poly(ethylene oxide)-Poly(propylene oxide)-Poly(ethylene oxide) Block Copolymer Studied by Cyclic Voltammetry

Yuanhua Ding, Ying Wang, and Rong Guo*

School of Chemistry & Chemical Engineering, Yangzhou University, Yangzhou, 225002, People's Republic of China

ABSTRACT: The cyclic voltammetric behaviors at a platinum electrode of an amphiphilic block copolymer [poly(ethylene oxide)-*block*-poly(propylene oxide)-*block*-poly(ethylene oxide) (F127)] in aqueous solutions were investigated. The mechanism of the electrochemical reaction of F127 at a platinum electrode was deduced. The diffusion coefficients of different-shaped aggregates formed by F127 were determined on this basis. The first and second critical micelle concentrations, corresponding to the formation of spherical micelles and the transition of the spherical to rod-like micelles, were 3.72×10^{-4} mol·L^{-1} and 1.49×10^{-3} mol·L^{-1}, respectively, which could be confirmed by the fluorescent anisotropy of pyrene in the F127 aggregates and the morphology of F127 micelles observed by freeze-fracture transmission electron microscopy.

Paper no. S1360 in *JSD 7*, 379–385 (October 2004).

KEY WORDS: Cyclic voltammetry, diffusion coefficient, PEO-PPO-PEO block copolymer, rod-like micelles, spherical micelles.

Amphiphilic block copolymers, and in particular poly(ethylene oxide)-*block*-poly(propylene oxide)-*block*-poly(ethylene oxide) (PEO-PPO-PEO) triblock copolymers (commercially available under the trade name Pluronic), can form different self-assembled structures [spherical micelles (1,2), rod-like micelles (3), as well as cubic, hexagonal, and lamellar lyotropic liquid crystals (4–7)] under appropriate conditions of copolymer concentration and/or temperature. Compared with the typical low-molecular-weight surfactants, Pluronic copolymers have superior properties, such as extremely low critical micelle concentrations (CMC), a large diversity in molecular characteristics (PPO/PEO ratio, molecular weight) and microstructures, and, as a result, rich amphiphilic properties (8) and a very low toxicity (9). PEO-PPO-PEO block copolymers have widespread industrial applications in biology, medicine, cosmetics, and textiles (10–12). Therefore, theoretical and practical research on the properties of Pluronic copolymers in aqueous solutions is arousing increasing interest (13,14). F127 is a typical amphiphilic triblock copolymer. Surface tension, light-scattering, small-angle neutron scattering, and nuclear magnetic resonance studies have been performed to understand its surface activity, interaction with normal surfactants, and the phase behaviors of its ternary systems with water and some organic compounds (14–19). However, little work has been done on the aggregation properties and micellar structural transitions of this kind of block copolymer by the electrochemical method, even though it is a very useful tool (20–23). In the present paper, the electrochemical behaviors of F127 in aqueous solutions are studied, and the mechanism of the electrochemical reaction of F127 at a platinum electrode is deduced by controlled-potential coulometry and *in situ* ultraviolet-visible (UV-vis) spectrometry. The diffusion coefficients of different-shaped aggregates are determined, and the aggregation properties of F127 are discussed.

EXPERIMENTAL PROCEDURES

Materials. F127 [HO–$(PEO)_x(PPO)_y(PEO)_x$–H, $x = 97$–106, $y = 65$–70] was obtained from BASF Co. (Florham Park, NJ). Pyrene (99%) was obtained from Fluka Co. (Buchs, Switzerland), and perchloric acid ($HClO_4$, A.R.) and sodium chloride (NaCl, A.R.) were from Shanghai Chemicals Co. (Shanghai, P.R. China). All the chemicals were used as received. Water was deionized and distilled.

Determination of the diffusion coefficient. Diffusion coefficients of different F127 aggregates in aqueous solutions were determined by cyclic voltammetry according to the electrochemical reaction of F127. In the three-electrode configuration, the working electrode was a 213-type platinum electrode (Shanghai Rex Instrument Factory), the auxiliary electrode was a platinum plate, and the reference electrode was a saturated calomel electrode (SCE; NaCl saturated, to avoid sedimentation of $KClO_4$). The added $HClO_4$ (0.10 mol·L^{-1}) had little effect on the micellization of nonionic surfactant F127 and was used as a supporting electrolyte. All the solutions were deoxygenated by bubbling them with nitrogen gas for 30 min before each measurement. The potential was swept linearly at 25 mV·s^{-1} between −0.20 and 1.30 V. The electrochemical experiments

*To whom correspondence should be addressed.
E-mail address: guorong@yzu.edu.cn

Abbreviations: CMC, critical micelle concentration; FF-TEM, freeze-fracture transmission electron microscopy; PEO, poly(ethylene oxide); PPO, poly(propylene oxide); SCE, saturated calomel electrode; UV-vis, ultraviolet-visible.

were conducted with the following apparatus: CHI630 electrochemical detector (CH Instruments Inc., Austin, TX), HPD-1A bipotentiostat (Yanbian Electrochemical Apparatus Co., Jilin, China), and 3086X-Y recorder (Sichuan Fourth Meters Co., China).

Determination of the mechanism of the electrochemical reaction. The mechanism for the electrochemical reaction of F127 in aqueous solution at the platinum electrode was deduced by controlled-potential coulometry, UV-vis spectroelectrochemistry, and the measurement of pH. In controlled-potential coulometry, the working electrode was a platinum gauze, the reference electrode was SCE (NaCl saturated), and the auxiliary electrode was a platinum plate. The solution of F127/$HClO_4$/H_2O was electrolyzed at a controlled potential of 1.209 V (vs. SCE) after deoxygenation with bubbling nitrogen for 30 min, and the solution of $HClO_4$/H_2O was electrolyzed at the same controlled potential and the same condition to eliminate the background current of the F127/$HClO_4$/H_2O system.

In UV-vis spectroelectrochemistry, the electrolysis cell was a thin-layer quartz cell (inner dimensions: $1.0 \times 0.2 \times 3.0$ cm), the working electrode was a platinum gauze, the auxiliary electrode was a platinum wire, and the reference electrode was an Ag/AgCl (NaCl saturated) electrode. Dissolved oxygen was removed from the solution by bubbling nitrogen through for 15 min before each measurement. The incident light was perpendicular to the working electrode, and the *in situ* UV-vis absorption spectra were recorded at wavelengths of 230–270 nm using a UV-2501 PC UV-vis spectrophotometer (Shimadzu Co., Kyoto, Japan). The electrolysis potentials were controlled in the range of 0.99–1.21 V (vs. Ag/AgCl), and the equilibrium electrolysis time was 5 min. The pH values were obtained with a pHS-25 pH meter (Shanghai Rex Instruments Factory).

Determination of the steady-state fluorescent anisotropy. The sample of F127 solution was excited with vertically polarized light, and the components of the emission intensity $I_{||}$ and $I_{\perp}$, corresponding to the polarized emission parallel and perpendicular to the direction of the polarized excitation, respectively, were determined by RF-5301 PC spectrofluorophotometer with polarization accessories (Shimadzu Co.). Then the steady-state fluorescent anisotropy r was calculated by the following equation (24):

$$r = \frac{I_{||} - I_{\perp}}{I_{||} + 2I_{\perp}} \qquad [1]$$

Pyrene was excited at 335 nm, and the emission was measured at 383 nm in the experiment.

Determination of the morphology of F127 micelles. The morphology of F127 micelles was directly observed by means of freeze-fracture transmission electron microscopy (FF-TEM). A small amount of micelle solution was placed on a 0.1-mm-thick copper disc. Then the copper disc was rapidly plunged into liquid nitrogen. The frozen samples were fractured and replicated in a BAF 400D freeze-etching apparatus (Bal-Tec, Balzer, Liechtenstein) at a sample temperature of −150°C and at a pressure of 2×10^{-6} mbar. The fracture plane was shadowed with platinum at an angle of 45° and with carbon at an angle of 90°. The replicas of the samples were examined using a Philips Tecnai-12 transmission electron microscope.

All measurements were carried out at 25 ± 0.1°C.

RESULTS AND DISCUSSION

Cyclic voltammetric behaviors of F127 in aqueous solution. Cyclic voltammograms of F127 in aqueous solution are presented in Figure 1. Except for trace *a* (the control, i.e., F127 is absent), oxidation peaks for F127 are present at 1.02 V. There are no corresponding reduction peaks except for an apparent cathodic peak at 0.48 V. We ascribed this cathodic peak to the reduction of PtO formed after the anodization above 0.7 V (vs. SCE) or in the pretreatment of the platinum electrode with hot, dilute HNO_3 solution and the H_2SO_4/$K_2Cr_2O_7$ solution (25). The oxidation peak potential of F127 shifted gradually from 1.02 to 1.19 V with the increase in scan rates. When the scan rate v_s is less than or equal to 30 mV·s^{-1}, the anodic peak current, i_a, is proportional to the square root of the scan rate (before point *a* in Fig. 2), and when v_s is greater than 30 mV·s^{-1} (after point *a* in Fig. 2), the i_a values deviate upward from the linear relation. Therefore, it follows that the electrochemical behavior of F127 at a platinum electrode is a diffusion-controlled irreversible process at low scan rates and that F127 is adsorbed on the electrode surface at high scan rates (26). Therefore, a low scan rate was employed in our study to reduce the adsorption of F127 on the electrode.

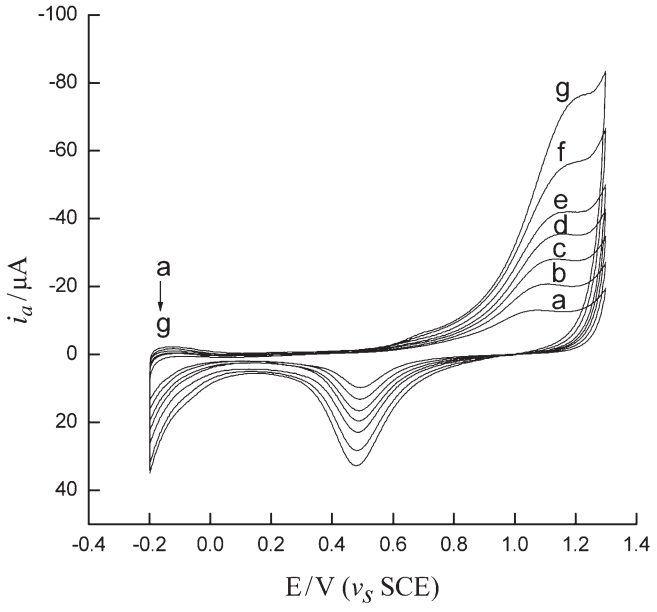

FIG. 1. The cyclic voltammograms of F127 (6.0×10^{-4} mol·L^{-1}) under different scan rates (v_s) at a platinum electrode. v_s (mV·s^{-1}): a. 10; b. 15; c. 20; d. 25; e. 30; f. 40; g. 50. SCE, standard calomel electrode.

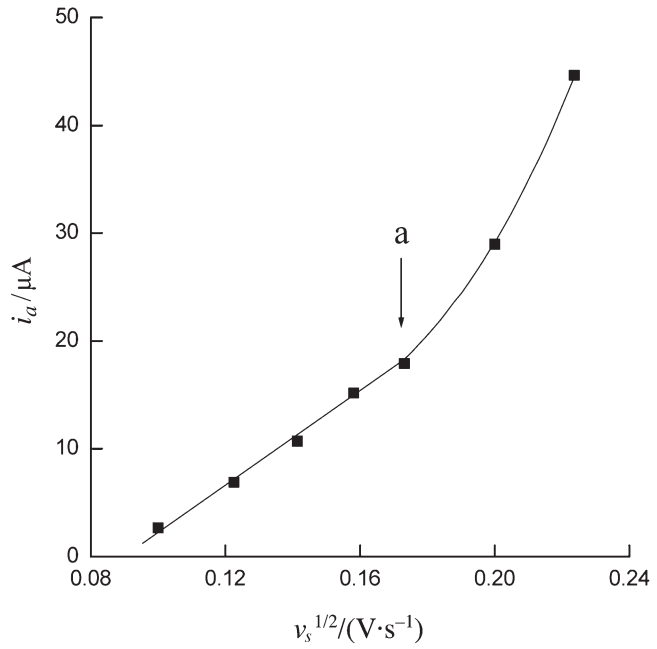

FIG. 2. The relation of peak current i_a with the square root of scan rate (v_s). Concentration of F127 (mol·L^{-1}): 6.0×10^{-4}; v_s/(mV·s^{-1}): 10–50.

Mechanism of the electrochemical reaction of F127. The molecular structure of F127 is as follows (Scheme 1):

$$HO\text{–}(CH_2CH_2O)_x\text{–}(\underset{\displaystyle CH_3}{\underset{|}{CHCH_2O}})_y\text{–}(CH_2CH_2O)_{x-1},\ x = 97\text{–}106,\ y = 65\text{–}70$$

SCHEME 1

In the usual situation, the alkyl and ether bonds in the F127 molecule are not easily oxidized, whereas the –OH group is relatively easily oxidized. Since the electrochemical oxidation of F127 at the platinum electrode is irreversible, the number of electrons transferred in the electrochemical reaction, n, can be determined through controlled-potential coulometry (27). The electrolysis current, i_t, decays exponentially with time according to the following relationship during the electrolysis (27):

$$i_t = i_0 e^{-pt} \qquad [2]$$

where i_0 is the initial current and p is the electrolytic rate constant. A straight line can be obtained by plotting log i_t vs. t, from which the slope p and the intercept i_0 are evaluated. With the assumption that the total quantity of electricity consumed in the electrolysis is Q_t, when $t \to \infty$, the value of Q_t at the completion of the electrolysis, Q_∞, is given by (27)

$$Q_\infty = i_0/p = nFVc_0 \qquad [3]$$

where n is the number of electrons transferred in the electrode reaction, F is the Faraday constant, V is the total solution volume, and c_0 is the initial concentration of the electroactive substance. From Equation 3, the value of Q_∞ can be first obtained, then the value of n. In the case of F127, the log i_t vs. t curve is shown in Figure 3; the number of electrons transferred in the electrode reaction is $n = 2.14 \approx 2$ after the background correction. The initial part of the log i_t vs. t curve deviates from the theoretical line, which is similar to that of the Mn^{2+} (25) and L-ascorbic acid (28) electrolyzed at a platinum gauze electrode at controlled potential. This deviation is attributed to the adsorption of a few F127 molecules on the electrode surface (25).

Figure 4 is the *in situ* UV absorption spectra of the electrochemical response for the F127 oxidation-reduction system. As shown in Figure 4, the reductive state of F127 does not absorb at 245 nm before electrolysis (Fig. 4, line a), whereas the oxidation product of F127 absorbs at 245 nm after electrolysis (Fig. 4, lines b–g). With the potential rising, the F127 concentration decreases; meanwhile, the concentration of the oxidation product increases, and the absorption intensity at 245 nm goes up gradually to a relatively stable state (Fig. 4, lines b–g). Furthermore, the absorption intensity at λ_{max} (245 nm) is rather low, which indicates that an $n \to \pi^*$ transition occurs in the oxidation product, so a carbonyl group may exist in the oxidation product (29). From the number of electrons ($n \approx 2$) and the UV absorption spectra, it was inferred that the oxidation product contained an aldehyde group. The pH value of the solution falls from 1.72 before electrolysis to 1.55 afterward, which suggests the generation of hydrogen ions by the electrode reaction. Based on the above analysis, a probable electrochemical mechanism of the F127 oxidation at the platinum electrode is deduced as follows:

$$RCH_2CH_2OH \rightarrow RCH_2CHO + 2H^+ + 2e^- \qquad [4]$$

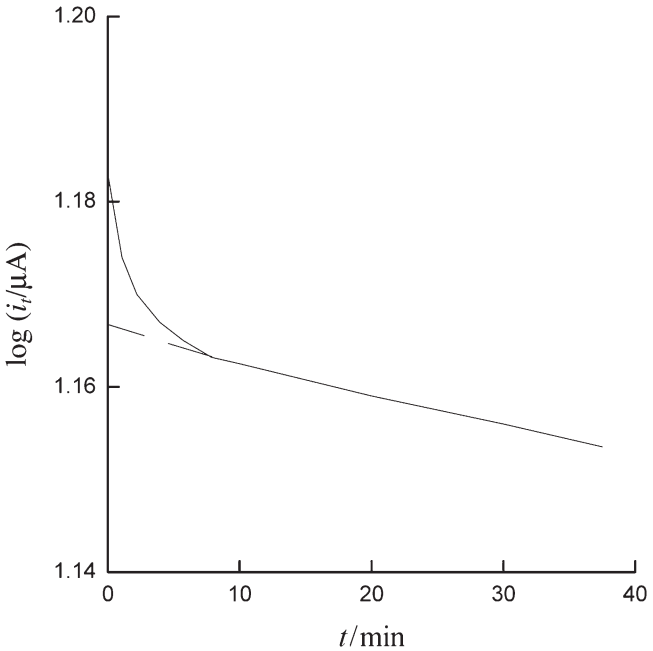

FIG. 3. The relation of log i_t with t for F127 under electrolysis at a platinum electrode. E = 1.209 V (vs. SCE). For abbreviation see Figure 1.

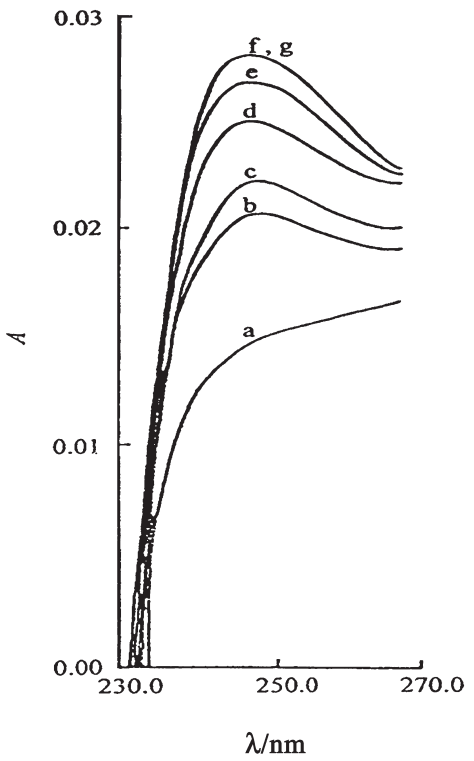

FIG. 4. The *in situ* UV absorption spectra for the F127 solution under controlled-potential electrolysis. Concentration of F127 (mol·L^{-1}): 7.9 × 10^{-4}; of $HClO_4$ (mol·L^{-1}): 0.10. *E* in V (vs. Ag/AgCl): a, not electrolyzed; b, 0.99; c, 1.07; d, 1.12; e, 1.15; f, 1.18; g, 1.21.

where

$$R = HO{-}(CH_2CH_2O)_x{-}(\underset{\displaystyle CH_3}{\underset{|}{CHCH_2O}})_y{-}(CH_2CH_2O)_{x-1}$$

This is in accordance with the electrode reaction of 1,4-butanediol ($HOH_2C{-}CH_2CH_2{-}CH_2OH$) at a platinum electrode, where 4-hydroxy butanal ($OHC{-}CH_2CH_2{-}CH_2OH$) is the main product (30).

Diffusion coefficient of F127/H_2O system. For a totally irreversible reaction, the relation of the diffusion coefficient *D* (cm^2·s^{-1}) with the peak current is given by Equation 5,

$$i_a = (2.99 \times 10^5)\, n(\alpha n_\alpha)^{1/2} A c^* D^{1/2} v_s^{1/2} \qquad [5]$$

where i_a is the anodic oxidation peak current at 25°C(A), *n* is the electron number for the electrode reaction ($n \approx 2$), α is the charge transfer coefficient, n_α is electron number for the rate-controlling step, *A* is the area of the electrode (cm^2), c^* is the bulk concentration of the solution (mol·cm^{-3}), and v_s is the scan rate (V·s^{-1}). The value of αn_α is given by Equation 6 (27),

$$\alpha n_\alpha = 47.7/(E_a - E_{a/2}) \qquad [6]$$

where E_a is the anodic peak potential (mV), and $E_{a/2}$ is the half-peak potential where the current is at half the peak value (mV). The diffusion coefficients of the F127/H_2O system are calculated by combining Equations 5 and 6.

The diffusion coefficients determined are the apparent ones, which consist of two parts,

$$D = fD_{free} + (1 - f)D_{mic} \qquad [7]$$

where $f = C_{free}/C_{total}$, and C_{free} and C_{total} are the concentrations of free and total F127, respectively. D_{free} and D_{mic} are the diffusion coefficients of F127 in the free and micellar states, respectively. The variation of diffusion coefficient *D* of F127 as a function of its concentration can reflect the transition of the microstructure of F127 aggregates. Similar studies have been reported using cyclic voltammetry on low-molecular-weight surfactants (20–23).

Figure 5 shows the relation of diffusion coefficients to F127 concentrations in a F127/H_2O system: *D* decreases with increasing F127 concentration and shows different trends in different concentration regions. The concentrations corresponding to the two intersection points are 3.72 × 10^{-4} and 1.49 × 10^{-3} mol·L^{-1}. The concentration at the first intersection point is very close to the CMC values obtained by the surface tension method (2.88 × 10^{-4} mol·L^{-1}) (15) and dye solubilization method (5.55 × 10^{-4} mol·L^{-1}) (2). According to the earlier determination of the first and second CMC for cetyl trimethylammonium bromide, sodium dodecyl sulfate, and Triton X-100 by cyclic voltammetry (20,21), the first intersection point in Figure 5, or 3.72 × 10^{-4} mol·L^{-1}, is the first CMC, and the second one, 1.49 × 10^{-3} mol·L^{-1}, should be the second CMC, namely, the concentration at which the spherical micelles transform into rod-like micelles. The first CMC obtained is in good

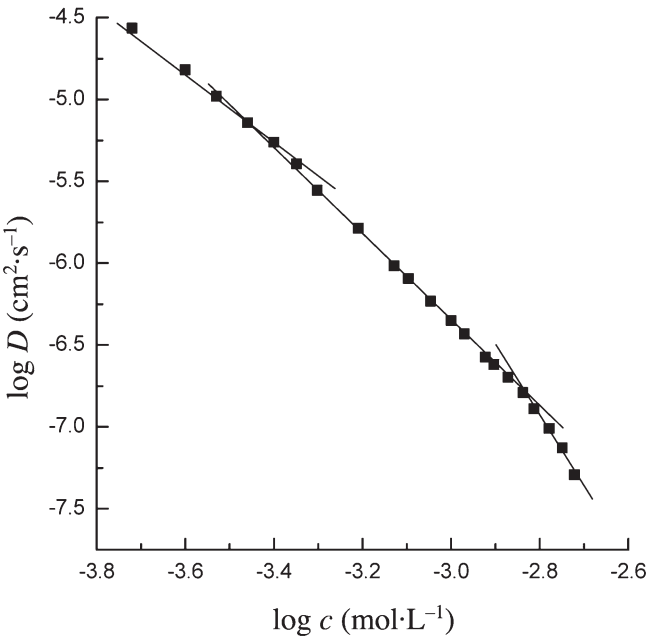

FIG. 5. The relation of log *D* with log *c* in the F127/H_2O system. *D*, diffusion.

agreement with the results in previous reports, but the second CMC of F127 has not been addressed so far in the literature.

It is obvious from Figure 5 that when the F127 concentration is below the first CMC, F127 molecules exist as monomers in various coiling forms, and the diffusion coefficient is greater. When the F127 concentration is above the first CMC, the F127 molecules exist as spherical micelles (3,31), and the micellar volume is greater than that of monomers. As a result, the spherical micelles diffuse more slowly, and D becomes smaller. And when the F127 concentration exceeds the second CMC, the micelles take on a rod-like structure (3), with even greater volume, and diffuse more slowly. Therefore, D becomes even smaller in comparison with that of spherical micelles.

To verify the transition from spherical to rod-like micelles, the steady-state fluorescent anisotropy of pyrene probe in F127 solution was measured, as shown in Figure 6. Under the conditions of given temperature (293.15 K) and fluorescent probe (32), the fluorescent anisotropy reflects the microviscosity of the microenvironment where the probe molecules are located, provides information on the micellar size and microstructure and correlates well with the CMC of surfactants. Komaromy-Hiller and Wandruszka (32) proved that the maximum fluorescent anisotropy of the probe corresponds to the CMC of a dilute solution of Triton X-114, which is a nonionic surfactant having the same ethylene oxide groups as F127. As shown in Figure 6, the fluorescent anisotropy appears to exhibit two maxima with increasing F127 concentration, the corresponding concentrations being 3.98×10^{-4} and 1.42×10^{-3} mol·L^{-1}, which is very consistent with the first and second CMC in Figure 5. When the F127 concentration approaches the first CMC, the PPO blocks in the F127 molecule tend to coil compactly, so the rotation of the probe molecule is inhibited, and as a result, the fluorescent anisotropy rises. This agrees with the changing tendency of the fluorescent polarization degree of the probe, 2-(4′-*N,N*-dimethylamino)-3-methoxyflavone, in micelles formed by structurally similar PEO-PPO-PEO triblock copolymer when its concentration is close to the CMC (33). When the F127 concentration reaches the first CMC, the probe molecule is located in the hydrophobic core formed by coiling PPO blocks (34), so the fluorescent anisotropy reaches the maximum. When the F127 concentration is above the first CMC, the micellar volume becomes greater with increasing F127 concentration. This provides more diffusion freedom for the solubilized probe molecule; therefore, the fluorescent anisotropy falls, which is similar to the case of the nonionic surfactant Triton X-114 after the formation of micelles (32). The number of micelles increases as the F127 concentration increases further (34). Since no remarkable change occurs in the microenvironment of the probe, there is no considerable variation in its fluorescent anisotropy. When the F127 concentration equals the second CMC, the F127 molecules form rod-like micelles driven by the hydrophobic interaction: The PPO blocks form the hydrophobic core along a certain direction, and the PEO blocks form the hydrophilic corona around the PPO core. This is similar to the formation of rod-like micelles of the diblock copolymer poly(ferrocenyldimethylsilane-*b*-dimethylsiloxane) (35). The degree of compactness of PPO blocks rises to a maximum again after the formation of rod-like micelles, and the fluorescent anisotropy of pyrene reaches a maximum again. Thereafter, with increasing F127 concentration, the aggregation number and the volume of the rod-like micelles increase further, so the diffusion freedom of the probe molecule increases again, and the fluorescent anisotropy falls. The results from Figure 6 confirm the validity of the first and second CMC of F127 as determined by cyclic voltammetry.

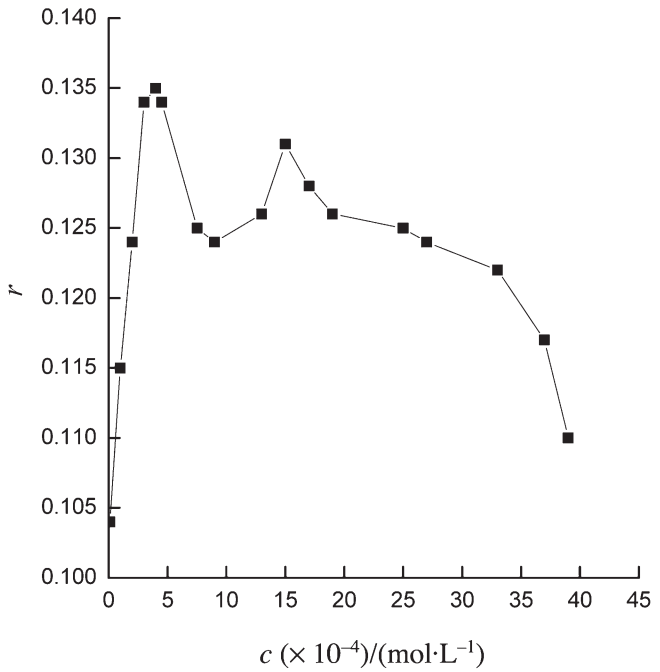

FIG. 6. The relation of the fluorescent anisotropy of pyrene in an F127/H_2O system with F127 concentration.

The transition from spherical to rod-like micelles was further proved by FF-TEM. As can be seen from Figure 7A, when the F127 concentration (4.00×10^{-4} mol·L^{-1}) is just above the first CMC, F127 form spherical micelles and the micellar size is from 15 to 35 nm. When the F127 concentration (1.70×10^{-3} mol·L^{-1}) is above the second CMC, F127 forms rod-like micelles with a diameter of about 35 nm (Fig. 7B). In addition, Figure 7B also indicates that rod-like and spherical micelles coexist when the F127 concentration is just above the second CMC. Therefore, the results of FF-TEM confirm the formation of rod-like micelles.

ACKNOWLEDGMENT

This work was supported by the Natural Scientific Foundation of China (No. 20233010).

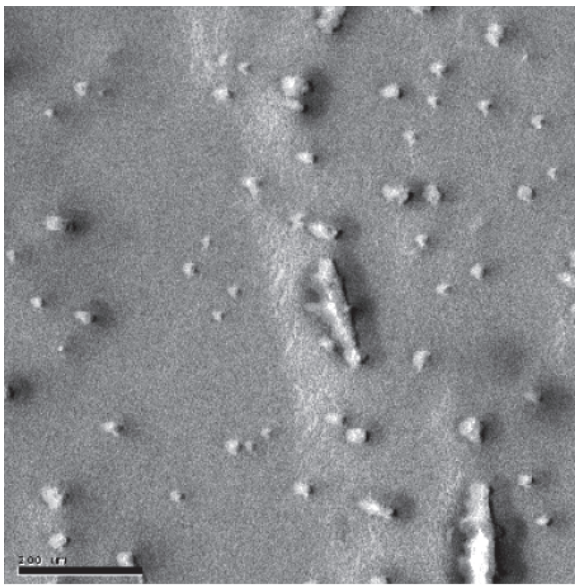

A

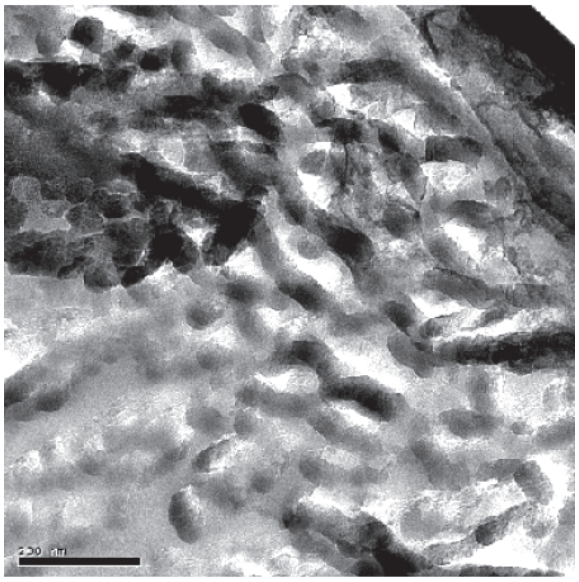

B

FIG. 7. Freeze-fracture electron micrographs of F127 micelles. Concentration of F127 (mol·L^{-1}): A, 4.00×10^{-4}; B, 1.70×10^{-3}. The scale bar is 200 nm.

REFERENCES

1. Malmsten, M., and B. Lindman, Self-assembly in Aqueous Block Copolymer Solutions, *Macromolecules 25*:5440 (1992).
2. Alexandridis, P., J.F. Holzwarth, and T.A. Hatton, Micellization of Poly(ethylene oxide)-Poly(propylene oxide)-Poly(ethylene oxide) Triblock Copolymers in Aqueous Solutions: Thermodynamics of Copolymer Association, *Macromolecules 27*:2414 (1994).
3. Almgren, M., W. Brown, and S. Hvidt, Self-aggregation and Phase Behavior of Poly(ethylene oxide)-Poly(propylene oxide)-Poly(ethylene oxide) Block Copolymers in Aqueous Solution, *Colloid Polym. Sci. 273*:2 (1995).
4. Alexandridis, P., D. Zhou, and A. Khan, Lyotropic Liquid Crystallinity in Amphiphilic Block Copolymers: Temperature Effects on Phase Behavior and Structure for Poly(ethylene oxide)-*b*-Poly(propylene oxide)-*b*-Poly(ethylene oxide) Copolymers of Different Composition, *Langmuir 12*:2690 (1996).
5. Zhou, D., P. Alexandridis, and A. Khan, Self-assembly in a Mixture of Two Poly(ethylene oxide)-*b*-Poly(propylene oxide)-*b*-Poly(ethylene oxide) Copolymers in Water, *J. Colloid Interface Sci. 183*:339 (1996).
6. Ivanova, R., B. Lindman, and P. Alexandridis, Effect of Glycols on the Self-assembly of Amphiphilic Block Copolymers in Water. 1. Phase Diagrams and Structure Identification, *Langmuir 16*:3660 (2000).
7. Holmqvist, P., P. Alexandridis, and B. Lindman, Modification of the Microstructure in Block Copolymer-Water-"Oil" Systems by Varying the Copolymer Composition and the "Oil" Type: A Small-Angle X-ray Scattering and Deuterium NMR Investigation, *J. Phys. Chem. B 102*:1149 (1998).
8. Alexandridis, P., and J.F. Holzwarth, Differential Scanning Calorimetry Investigation of the Effect of Salts on Aqueous Solution Properties of an Amphiphilic Block Copolymer (Poloxamer), *Langmuir 13*:6074 (1997).
9. Bohorquez, M., C. Koch, T. Trygstad, and N. Pandit, A Study of the Temperature-Dependent Micellization of Pluronic F127, *J. Colloid Interface Sci. 216*:34 (1999).
10. Bhardwaj, R., and J. Blanchard, Controlled-Release Delivery System for the α-MSH Analog Melanotan-I Using Poloxamer 407, *J. Pharm. Sci. 85*:915 (1996).
11. Ivanova, R., B. Balinov, R. Sedev, and D. Exerowa, Formation of a Stable, Highly Concentrated O/W Emulsion Modeled by Means of Foam Films, *Colloids Surf. A 149*:23 (1999).
12. Luo, Y.Z., C.V. Nicholas, D. Attwood, J.H. Clooett, C. Price, C. Booth, B. Chu, and Z.K. Zhou, *block*-Copoly(oxyethylene/oxybutylene/oxyethylene), $E_{40}B_{15}E_{40}$, in Aqueous Solution: Micellisation, Gelation and Drug Release, *J. Chem. Soc. Faraday Trans. 89*:539 (1993).
13. Kostarelos, K., P.F. Luckham, and T.F. Tadros, Addition of (tri)Block Copolymers to Phospholipid Vesicles: A Study of the Molecular Morphology and Structure by Using Hydrophobic Dye Molecules as Bilayer Probes, *J. Colloid Interface Sci. 191*:341 (1997).
14. Li, Y., R. Xu, S. Conderc, D.M. Bloor, E. Wyn-Jones, and J.F. Holzwarth, A Small-Angle Neutron Scattering Study of Spherical and Wormlike Micelles Formed by Poly(oxyethylene)-Based Diblock Copolymers, *Langmuir 17*:183 (2001).
15. Wanka, G., H. Hoffmann, and W. Ulbricht, The Aggregation Behavior of Poly(oxyethylene)-Poly(oxypropylene)-Poly(oxyethylene)-*block*-Copolymers in Aqueous Solution, *Colloid Polym. Sci. 268*:101 (1990).
16. Ghoreishi, S.M., G.A. Fox, D.M. Bloor, J.F. Holzwarth, and E. Wyn-Jones, EMF and Microcalorimetry Studies Associated with the Binding of the Cationic Surfactants to Neutral Polymers, *Langmuir 15*:5474 (1999).
17. Li, Y., R. Xu, D.M. Bloor, J.F. Holzwarth, and E. Wyn-Jones, The Binding of Sodium Dodecyl Sulfate to the ABA Block Copolymer Pluronic F127 ($EO_{97}PO_{69}EO_{97}$): An Electromotive Force, Microcalorimetry, and Light Scattering Investigation, *Langmuir 16*:10515 (2000).
18. Holmqvist P., P. Alexandridis, and B. Lindman, Phase Behavior and Structure of Ternary Amphiphilic Block Copolymer-Alkanol-Water Systems: Comparison of Poly(ethylene oxide)/Poly(propylene oxide) to Poly(ethylene oxide)/Poly(tetrahydrofuran) Copolymers, *Langmuir 13*: 2471 (1997).
19. Ivanova, R., B. Lindman, and P. Alexandridis, Evolution in Structural Polymorphism of Pluronic F127 Poly(ethylene oxide)-Poly(propylene oxide) Block Copolymer in Ternary Systems with Water and Pharmaceutically Acceptable Organic Solvents: From "Glycols" to "Oils", *Langmuir 16*: 9058 (2000).

20. Liu, T.Q., R. Guo, M. Shen, and W.L. Yu, Determination of the Diffusion Coefficients of Micelle and the First CMC and Second CMC in SDS and CTAB Solution, *Acta Physico-Chim. Sinica 12*:337 (1996).
21. Guo, R., Y.H. Ding, and T.Q. Liu, Diffusion Coefficient and Structural Properties in Triton X-100/*n*-C_4H_9OH/H_2O System, *Acta Chim. Sinica 57*:943 (1999).
22. Asakawa, T., H. Sunagawa, and S. Miyagishi, Diffusion Coefficients of Micelles Composed of Fluorocarbon Surfactants with Cyclic Voltammetry, *Langmuir 14*:7091 (1998).
23. Hassan, P.A., and J.V. Yakhmi, Growth of Cationic Micelles in the Presence of Organic Additives, *Langmuir 16*:7187 (2000).
24. Lakowicz, J.R., *Principles of Fluorescence Spectroscopy*, Plenum Press, New York, 1983, p. 112.
25. Harrar, J.E., Technique, Apparatus, and Analytical Applications of Controlled-Potential Coulometry, in *Electroanalytical Chemistry*, edited by A. J. Bard, Marcel Dekker, New York, 1975, vol. 8, p. 91.
26. Gao, X.X., (ed.), *Introduction to the Electroanalytical Chemistry*, Science Press, Beijing, 1986, p. 310.
27. Bard, A.J., and L.R. Faulkner, *Electrochemical Methods: Fundamentals and Applications*, John Wiley & Sons, New York, 1980, p. 222.
28. Santhanam, K.S.V., and V.R. Krishnan, Estimation of Ascorbic Acid by Controlled Potential Coulometry, *Anal. Chem. 33*:1493 (1961).
29. Ning, Y.C., *Structure Identification of Organic Compound and Organic Spectroscopy*, Science Press, Beijing, China, 2001, p. 368.
30. Hilmi, A., E.M. Belgsir, and J.M. Léger, Electrocatalytic Oxidation of Aliphatic Diols Part V: Electro-oxidation of Butanediols on Platinum Based Electrodes, *J. Electroanal. Chem. 435*:69 (1997).
31. Bahadur, P., and K. Pandya, Aggregation Behavior of Pluronic P-94 in Water, *Langmuir 8*:2666 (1992).
32. Komaromy-Hiller, G., and R. Wandruszka, Anisotropy Changes of a Fluorescent Probe During the Micellar Growth and Clouding of a Nonionic Detergent, *J. Colloid Interface Sci. 177*:156 (1996).
33. Zhang, Y.H., S.K. Wu, and P.C. Huang, The Block Architecture Effect on the Association Propertites of Amphiphilic Block Copolymers in Aqueous Solution, *Acta Polymer. Sinica 3*:332 (1998).
34. Almgren, M., P. Bahadur, M. Jansson, P. Li, W. Brown, and A. Bahadur, Static and Dynamic Properties of a (PEO-PPO-PEO) Block Copolymer in Aqueous Solution, *J. Colloid Interface Sci. 151*:157 (1992).
35. Massey, J.A., K. Temple, L. Cao, Y. Rharbi, J. Raez, M.A. Winnik, and I. Manners, Self-Assembly of Organometallic Block Copolymers: The Role of Crystallinity of the Core-Forming Polyferrocene Block in the Micellar Morphologies Formed by Poly(ferrocenylsilane-*b*-dimethylsiloxane) in *n*-Alkane Solvents, *J. Am. Chem. Soc. 122*:11577 (2000).

[Received February 28, 2004; accepted May 10, 2004]

Yuanhua Ding is an associate professor in the School of Chemistry and Chemical Engineering at Yangzhou University. He received his M.S. degree in physical chemistry from Yangzhou University in 1999 and is working toward his Ph.D. in physical chemistry. His research is in the area of physical chemistry of surfactants.

Ying Wang obtained her M.S. degree in physical chemistry from Yangzhou University in 2003, and she is working toward her Ph.D at the Chinese Academy of Sciences.

Dr. Rong Guo is a professor in the School of Chemistry and Chemical Engineering at Yangzhou University. He is the president of Yangzhou University, chairman of the Committee of Colloid and Interface Chemistry Division in China, and the regional editor for the Journal of Dispersion Science and Technology. *He received his Ph.D. degree in physical chemistry from Clarkson University (Potsdam, NY) in 1999. His current research topic is the physical chemistry of surfactants.*